



ARTICLE OPEN



IKK α promotes lung adenocarcinoma growth through ERK signaling activation via DARPP-32-mediated inhibition of PP1 activity

Sk. Kayum Alam¹ , Li Wang¹, Zhu Zhu¹ and Luke H. Hoepfner^{1,2} 

Non-small cell lung cancer (NSCLC) accounts for 80–85% cases of lung cancer cases. Diagnosis at advanced stages is common, after which therapy-refractory disease progression frequently occurs. Therefore, a better understanding of the molecular mechanisms that control NSCLC progression is necessary to develop new therapies. Overexpression of I κ B kinase α (IKK α) in NSCLC correlates with poor patient survival. IKK α is an NF- κ B-activating kinase that is important in cell survival and differentiation, but its regulation of oncogenic signaling is not well understood. We recently demonstrated that IKK α promotes NSCLC cell migration by physically interacting with dopamine- and cyclic AMP-regulated phosphoprotein, Mr 32000 (DARPP-32), and its truncated splice variant, t-DARPP. Here, we show that IKK α phosphorylates DARPP-32 at threonine 34, resulting in DARPP-32-mediated inhibition of protein phosphatase 1 (PP1), subsequent inhibition of PP1-mediated dephosphorylation of ERK, and activation of ERK signaling to promote lung oncogenesis. Correspondingly, IKK α ablation in human lung adenocarcinoma cells reduced their anchorage-independent growth in soft agar. Mice challenged with IKK α -ablated HCC827 cells exhibited less lung tumor growth than mice orthotopically administered control HCC827 cells. Our findings suggest that IKK α drives NSCLC growth through the activation of ERK signaling via DARPP-32-mediated inhibition of PP1 activity.

npj Precision Oncology (2023)7:33; <https://doi.org/10.1038/s41698-023-00370-3>

INTRODUCTION

Lung cancer is the second most frequently diagnosed cancer in both men and women and the leading cause of cancer-related deaths worldwide, with an estimated 2.2 million new cases and 1.8 million deaths per year^{1,2}. Non-small cell lung cancer (NSCLC) is the most common type of lung cancer and accounts for 85% of total diagnoses³. Substantial improvements in the application of predictive biomarkers, smoking cessation, and modification of current treatment paradigms have led to notable progress in managing NSCLC and have transformed outcomes for many patients^{4–6}. However, the 5-year relative survival of lung cancer patients is dismal (22.9%) due to the emergence of therapy-resistant disease and metastasis^{7,8}. Therefore, improving the general understanding of disease biology, implementing screening programs to diagnose patients early, and identifying alternative treatment strategies to circumvent treatment-refractory disease progression is required to improve the lung cancer survival rate. Here, we introduce a new mechanism for the molecular regulation of oncogenic signaling that builds upon current knowledge of lung cancer biology and may inform the development of novel anticancer therapies.

I κ B (inhibitor of nuclear factor kappa B) kinase α (IKK α), a serine/threonine protein kinase, is encoded by the conserved helix-loop-helix ubiquitous kinase (*CHUK*) gene⁹. Phosphorylation of I κ B α , a nuclear factor- κ B (NF- κ B) inhibitor, by IKK α and IKK β , catalytical subunits of the IKK complex, promotes I κ B α protein degradation, which initiates nuclear translocation of NF- κ B dimers. In the nucleus, NF- κ B functions as a transcription factor to regulate immunity, infection, lymphoid organ/cell development, cell death/growth, and tumorigenesis^{9–13}. In noncanonical signaling, NF- κ B-inducing kinase activates IKK α protein via phosphorylation

upon activation of upstream membrane-bound receptors by their cognate ligands. Active IKK α then phosphorylates and cleaves the p100 protein to generate p52, which complexes with the RelB NF- κ B subunit, resulting in nuclear translocation of the p52/RelB dimer to regulate several immune functions, including lymphoid organ development, the priming function of dendritic cells, B-cell survival, generation, and maintenance of effector- and memory-T cells, and antiviral innate immunity^{9,14,15}.

The tumor-promoting role of IKK α has been documented in breast, prostate, nonmelanoma skin, and lung cancer^{16–18}. Aberrant overexpression of IKK α protein is associated with decreased patient survival and promotes the growth of lung adenocarcinoma; it may therefore be used as a biomarker to predict clinical response in lung adenocarcinoma patients¹⁹. In a separate study, investigators showed that overexpression of cytosolic and nuclear IKK α protein promotes NSCLC cell proliferation, survival, and migration by activating the ERK, p38/MAPK, and mammalian target of rapamycin (mTOR) cell signaling pathways. Additionally, activation of protumorigenic cell signaling pathways depends on the subcellular localization of IKK α ¹⁸. Although the role of IKK α in promoting cancer has been well established in the context of lung cancer driven by *Kras*-activating mutations, it may have tumor-suppressing activity: in a *Kras*^{G12D}-driven spontaneous mouse model of NSCLC, lung-specific *Ikka* deletion induced by intratracheally injected adenovirus-Cre recombinase promoted NSCLC initiation and growth by elevating the expression of inflammatory cytokines and chemokines, including NF- κ B targets²⁰. We sought to understand the role of IKK α protein overexpression in tumor growth and progression in *Kras*-wild-type NSCLC.

¹The Hormel Institute, University of Minnesota, Austin, MN, USA. ²Masonic Cancer Center, University of Minnesota, Minneapolis, MN, USA. ✉email: skalam@umn.edu; hoepf005@umn.edu

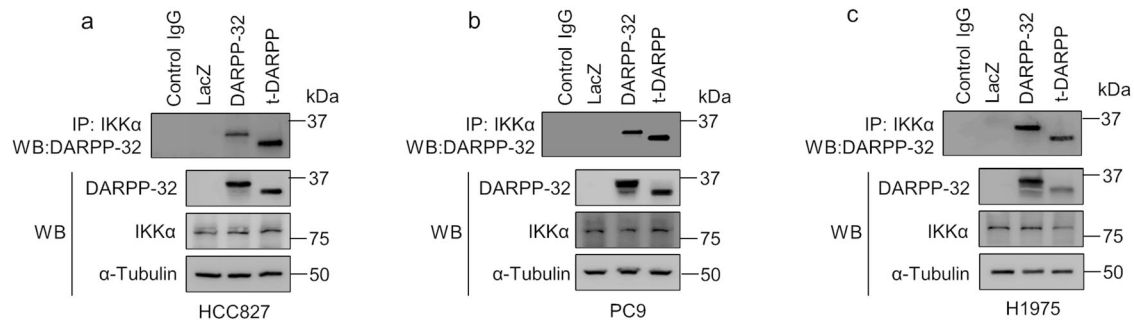


Fig. 1 IKKα physically associates with DARPP-32 isoforms. **a–c** Human lung adenocarcinoma cell lines HCC827 (**a**), PC9 (**b**), and H1975 (**c**) stably overexpressing FLAG-tagged human DARPP-32 isoforms were lysed and subjected to immunoprecipitation using anti-IKKα antibodies. Immunoprecipitated lysates were separated in SDS-PAGE and immunoblotted with antibodies against IKKα, FLAG (that detects exogenously overexpressed DARPP-32), and α-tubulin (loading control).

Dopamine- and cyclic AMP-regulated phosphoprotein, Mr 32000 (DARPP-32), is primarily expressed in the brain, including the caudate nucleus, cerebral cortex, and striatum. It acts as a downstream signaling molecule through dopamine receptor 1 (D₁R) and is negatively regulated by dopamine receptor 2 (D₂R) and glutamate signaling^{21–23}. Phosphorylation of DARPP-32 in response to cAMP in dopamine-responsive nerve tissue attenuates protein phosphatase 1 (PP1) activity, affecting the regulation of several cell signaling pathways²⁴. Although expression of DARPP-32 proteins is typically restricted to neuronal cell types in the brain, DARPP-32 and its truncated isoform t-DARPP are aberrantly overexpressed in many types of cancer, including lung cancer^{25–31}. t-DARPP, which was originally discovered in gastric cancer tissues, lacks the N-terminal domain responsible for modulating PP1 function²⁸. It is phosphorylated by cyclin-dependent kinase (CDK) 1 and 5 and activates protein kinase A (PKA), thereby conferring resistance to trastuzumab, a HER2-targeted anticancer agent, via sustained signaling through the phosphatidylinositol-4,5-bisphosphate 3-kinase (PI3K)/AKT pathway^{32,33}. Since this discovery, the DARPP-32 and t-DARPP isoforms overexpressed in breast, colon, esophageal, gastric, pancreas, prostate, lung, and ovarian cancer tissues have been shown to activate robust anti-apoptotic signaling through the activation of the AKT and ERK cell signaling pathways; to increase metabolism by forming a complex with the insulin-like growth factor 1 receptor (IGF1R); and to promote cell survival in the presence of receptor tyrosine kinase inhibitors, including gefitinib and trastuzumab^{25–27,29,30,34–37}. Our previous work, which serves as the rationale for this current study, revealed that DARPP-32 isoforms increase NSCLC cell migration via increasing the expression of NF-κB2-controlled migratory genes by establishing a direct physical interaction with IKKα²⁵. However, the precise role of the DARPP-32/IKKα complex in regulating NSCLC progression has yet to be determined.

In this study, we report that the IKKα protein inhibits PP1 function through phosphorylation of the full-length DARPP-32 protein at the Thr-34 position. Pharmacologic inhibition of PP1 activates ERK cell signaling pathways, leading to NSCLC growth promotion in vitro. Furthermore, we show in an orthotopic mouse model that depletion of IKKα protein reduces NSCLC growth. Taken together, our findings suggest that IKKα protein directly phosphorylates full-length DARPP-32 protein to stimulate oncogenic kinase activity through the inhibition of PP1 function to promote NSCLC growth and oncogenesis.

RESULTS

Phosphorylation of DARPP-32 at Thr-34 is regulated by IKKα

Given our prior observation that the physical association between IKKα and DARPP-32 promotes NSCLC cell migration²⁵, we

postulated that DARPP-32 can be phosphorylated by the kinase function of IKKα. To test our hypothesis, we first performed immunoprecipitation experiments in three human NSCLC cell lines, HCC827, PC9, and H1975, which confirmed that IKKα establishes a direct physical interaction with DARPP-32 (Fig. 1a–c). We next performed nonradioactive in vitro kinase assays using commercially available kinase-active IKKα protein. Briefly, DARPP-32 and its short isoform, t-DARPP, were purified from lysates of four different human lung adenocarcinoma cell lines, A549, HCC827, PC9, and H1975, using anti-FLAG M2 affinity beads and then incubated with purified IKKα protein in kinase assay buffers containing ATP. Reaction end products were subjected to immunoblotting with anti-phospho DARPP-32 (both T34 and T75) and -total DARPP-32 antibodies. Our western blotting results confirm that purified full-length DARPP-32 protein (but not t-DARPP) serves directly as a substrate for IKKα (Fig. 2a, b). Based on our results, it is evident that IKKα phosphorylates full-length DARPP-32 protein at the Thr-34 position (Fig. 2a, b). As expected, IKKα does not phosphorylate t-DARPP because the Thr-34 residue is absent in t-DARPP protein since t-DARPP lacks the first 36 amino acids present in full-length DARPP-32 protein (Fig. 2a, c). However, the presence of strong signals on the immunoblot using anti-phospho DARPP-32 (T75) suggests that t-DARPP is phosphorylated at Thr-75 by an unknown endogenous kinase(s) (Fig. 2a, c). In summary, our results indicate that IKKα physically associates with DARPP-32 protein and phosphorylates full-length DARPP-32 protein at the Thr-34 position. While our findings suggest that full-length DARPP-32 protein is not phosphorylated at Thr-75 by IKKα, we were unable to test whether IKKα phosphorylates DARPP-32 at positions other than Thr-34 due to the lack of availability of anti-phospho DARPP-32 antibodies specific for other sites.

Increased expression of p-ERK is regulated by IKKα via DARPP-32/PP1α signaling

A seminal report suggested that the neuronal phosphoprotein DARPP-32 acts as a potent inhibitor of PP1 following phosphorylation by PKA at the Thr-34 position²⁴. On the basis of this report, we hypothesized that IKKα-mediated DARPP-32 phosphorylation inhibits PP1α activity in NSCLC cells and promotes oncogenic growth by activating cell signaling pathways. To test our hypothesis, we transiently overexpressed constitutively active and kinase-dead IKKα plasmids in HCC827 and H1650 cells and performed an immunoblotting experiment with antibodies directed against phosphorylated DARPP-32 (T34). In line with our previous in vitro kinase results, we observed that expression of phosphorylated DARPP-32 increases to a greater extent in HCC827 and H1650 cell lysates overexpressing active IKKα than in GFP- or kinase-dead IKKα-expressing cell lysates (Fig. 3a, b). Phosphorylation of PP1α by cdc2 kinases in NIH-3T3 cells inhibits PP1α phosphatase activity in a cell cycle-dependent manner³⁸, and

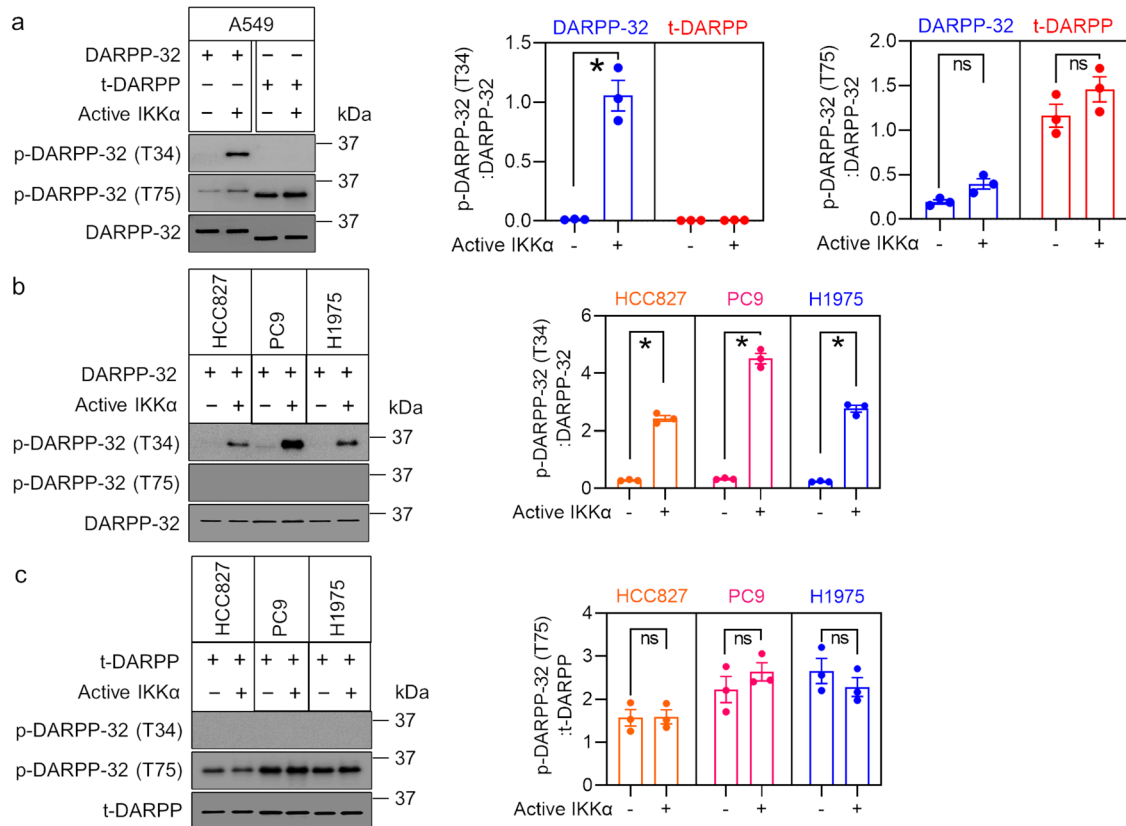


Fig. 2 IKK α phosphorylates DARPP-32 at Thr-34. **a** Human A549 cell lines stably overexpressing FLAG-tagged human DARPP-32 isoforms (DARPP-32 and t-DARPP) were lysed and subjected to immunoprecipitation using anti-FLAG antibody-conjugated agarose beads. Immunoprecipitated lysates were used to perform nonradioactive in vitro kinase assays following incubation with commercially available active IKK α protein. At the end, the reaction mixtures were subjected to immunoblotting using antibodies against DARPP-32 phosphorylated on Thr-34 or Thr-75 and total DARPP-32 protein. **b, c** Human HCC827, PC9, and H1975 lung adenocarcinoma cell lines retrovirally transduced with either FLAG-tagged human DARPP-32 (**b**) or t-DARPP (**c**) cDNA plasmids were lysed, immunoprecipitated, incubated with active IKK α protein, and subjected to western blotting using anti-phospho (Thr-34 or Thr-75) DARPP-32 and anti-DARPP-32 antibodies. Data from one experimental replicate are shown. The experiments were repeated three times independently; each circle in a bar represents one experiment. Error bars indicate SEM. * $P < 0.05$; ns not significant.

phosphorylation of DARPP-32 at the T34 position leads to DARPP-32-mediated phosphorylation and inactivation of PP1 α in neurons and cancer cells^{24,39}. We, therefore, sought to determine the effect of IKK α expression on the levels of inactive PP1 α protein in immunoblotting experiments using anti-phospho PP1 α antibodies. Expression of phosphorylated (inactive) PP1 α proteins increases in stable DARPP-32-overexpressed NSCLC cells upon transient expression of constitutively active IKK α cDNA plasmids compared to GFP- or kinase-dead IKK α - expression plasmids (Fig. 3a, b). As expected, transfection of constitutively active IKK α cDNA plasmids in T34A DARPP-32-overexpressed HCC827 and H1650 cells shows no increase in phosphorylated PP1 α expression (Supplementary Fig. 1a, b). Collectively, our findings suggest that overexpression of IKK α leads to increased DARPP-32 phosphorylation at the T34, which inhibits PP1 phosphatase activity. To test how repression of PP1 function by the IKK α /DARPP-32 complex stimulates downstream oncogenic cell signaling, we focused on the ERK/MAPK signaling pathway because pharmacologic inhibition of PP1 activity has been reported to increase ERK activity⁴⁰. In immunoblotting experiments, we observed an increase in the expression of phosphorylated ERK in HCC827 and H1650 cells exogenously expressing constitutively active IKK α compared to GFP- or kinase-dead IKK α - transfected cells (Fig. 3a, b), whereas phosphorylated ERK expression remains unchanged upon transient expression of constitutively active IKK α cDNA plasmids in stable T34A DARPP-32-overexpressed HCC827 and H1650 cells

(Supplementary Fig. 1a, b). To validate our theory that phosphorylation of ERK protein is controlled by PP1 α phosphatase, we performed western blotting experiments in HCC827 and H1650 cells treated with a pharmacological inhibitor of PP1 α , calyculin A. The expression of phosphorylated (i.e., inactive) PP1 α , as well as phosphorylated (i.e., activated) ERK, was higher in calyculin A-treated HCC827 and H1650 cells than in vehicle-treated cells (Fig. 3c, d). Calyculin A is also known to inhibit PP2a activity, which represents a limitation of our current studies. Future similar experiments specifically ablating PP1 α using shRNA or CRISPR are warranted to definitively confirm whether phosphorylation of ERK protein is controlled by PP1 α phosphatase as our initial data suggests. In summary, our results suggest that overexpression of kinase-active IKK α protein positively regulates the ERK-MAPK pathway through the DARPP-32/PP1 α axis.

IKK α controls the inhibition of PP1 α phosphatase activity

To test our hypothesis that IKK α prevents PP1 α phosphatase activity in NSCLC cells by phosphorylating DARPP-32 at Thr-34, we performed an in vitro phosphatase assay in lung adenocarcinoma cells stably overexpressing DARPP-32 protein. Briefly, kinase-dead, full-length, and constitutively active IKK α plasmids, as well as GFP-expressing control plasmids, were transiently transfected into HCC827 and H1650 cells stably overexpressing DARPP-32 protein. Endogenous PP1 α was immunoprecipitated from the cell lysates and subjected to phosphatase assays. We observed decreased

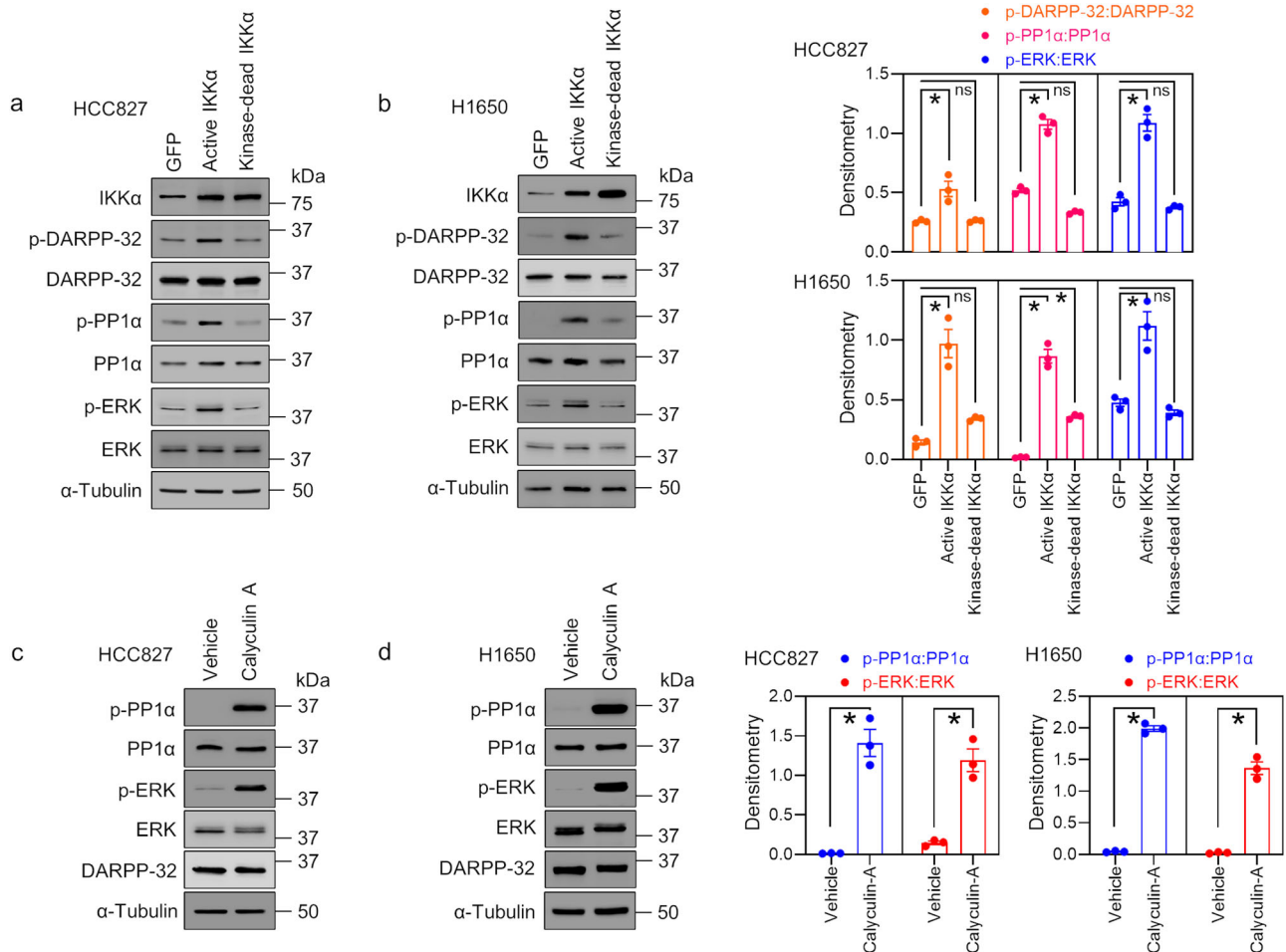


Fig. 3 Overexpression of constitutively active IKK α activates ERK signaling. **a, b** Human lung cancer cells, HCC827 (**a**) and H1650 (**b**), transfected with GFP (control), constitutively active IKK α , or kinase-dead IKK α were lysed using 1 \times RIPA buffer supplemented with protease and phosphatase inhibitors. Equal amounts of proteins were separated with 4–20% SDS-PAGE and transferred to polyvinylidene difluoride membranes. Antigen-coated membranes were incubated overnight with primary antibodies against IKK α , phosphorylated DARPP-32 (Thr-34), total DARPP-32, phosphorylated PP1 α (Thr320), total PP1 α , phosphorylated ERK (Thr202/Tyr204), total ERK, and α -tubulin (loading control). **c, d** Vehicle (DMSO)- or calyculin A-treated human HCC827 (**c**) and H1650 (**d**) cells were lysed with 1 \times RIPA buffer and subjected to immunoblotting using anti-phospho PP1 α (Thr320), -total PP1 α , -phospho ERK (Thr202/Tyr204), -total ERK, -DARPP-32, and - α -tubulin (loading control) antibodies. Chemiluminescence signals were detected after incubating membranes with HRP-tagged secondary antibodies. Representative images from one experiment are shown, but results were validated by performing three independent biological repeats. Bar graphs at the right show quantification of the results from the three western blotting experiments. Error bars indicate SEM. * $P < 0.05$; ns not significant.

PP1 α phosphatase activity (i.e., lower concentrations of released phosphates) in the lysates of cells overexpressing full-length or kinase-active IKK α relative to lysates of GFP-expressing cells (Fig. 4a, b). As expected, overexpression of kinase-dead IKK α in both cell lines failed to inhibit PP1 α phosphatase activity (Fig. 4a, b). To further test whether IKK α blocks PP1 α phosphatase activity via DARPP-32 phosphorylation at Thr-34, we stably overexpressed mutant DARPP-32 (T34A) in HCC827 and H1650 cells and repeated the *in vitro* phosphatase assay. As expected, no inhibition of PP1 α activity was seen in cells overexpressing full-length or constitutively active IKK α in the presence of mutant DARPP-32 (Fig. 4c, d). To ensure that equal amounts of immunoprecipitated PP1 α were used in the *in vitro* phosphatase assay, we performed immunoblotting experiments to measure the expression level of PP1 α in different groups. We observed that equal amounts of PP1 α were immunoprecipitated in HCC827 and H1650 cells exogenously expressing kinase-dead, full-length, or constitutively active IKK α or GFP (Fig. 4e–h). Taken together, our findings indicate that IKK α -mediated DARPP-32 phosphorylation inhibits PP1 α phosphatase activity.

Depletion of IKK α expression in tumor cells inhibits oncogenic growth advantage

To test the premise that IKK α promotes oncogenic tumor growth, we first performed soft agar anchorage-independent growth assays in human lung adenocarcinoma HCC827, PC9, and H1650 cells because anchorage-independent growth is considered one of the most reliable markers of malignant transformation⁴¹. We observed less anchorage-independent growth (number of colonies formed on the soft-agar plates) of HCC827, PC9, and H1650 cells transduced with IKK α shRNAs relative to corresponding LacZ shRNA-transduced controls (Fig. 5a, b). We next performed immunoblotting experiments to investigate molecular mechanisms of IKK α -mediated oncogenic tumor growth. Upon knock-down of IKK α , we observed decreased expression of each of phosphorylated DARPP-32 at Thr-34 (i.e., reduced activity), -PP1 α (i.e., increased activity), and -ERK (i.e., reduced activity) compared to LacZ shRNA-transduced control cells (Fig. 5c, d), suggesting that IKK α promotes anchorage-independent oncogenic lung tumor growth through regulation of the DARPP-32/PP1 α /ERK cell signaling pathway. We previously showed that DARPP-32

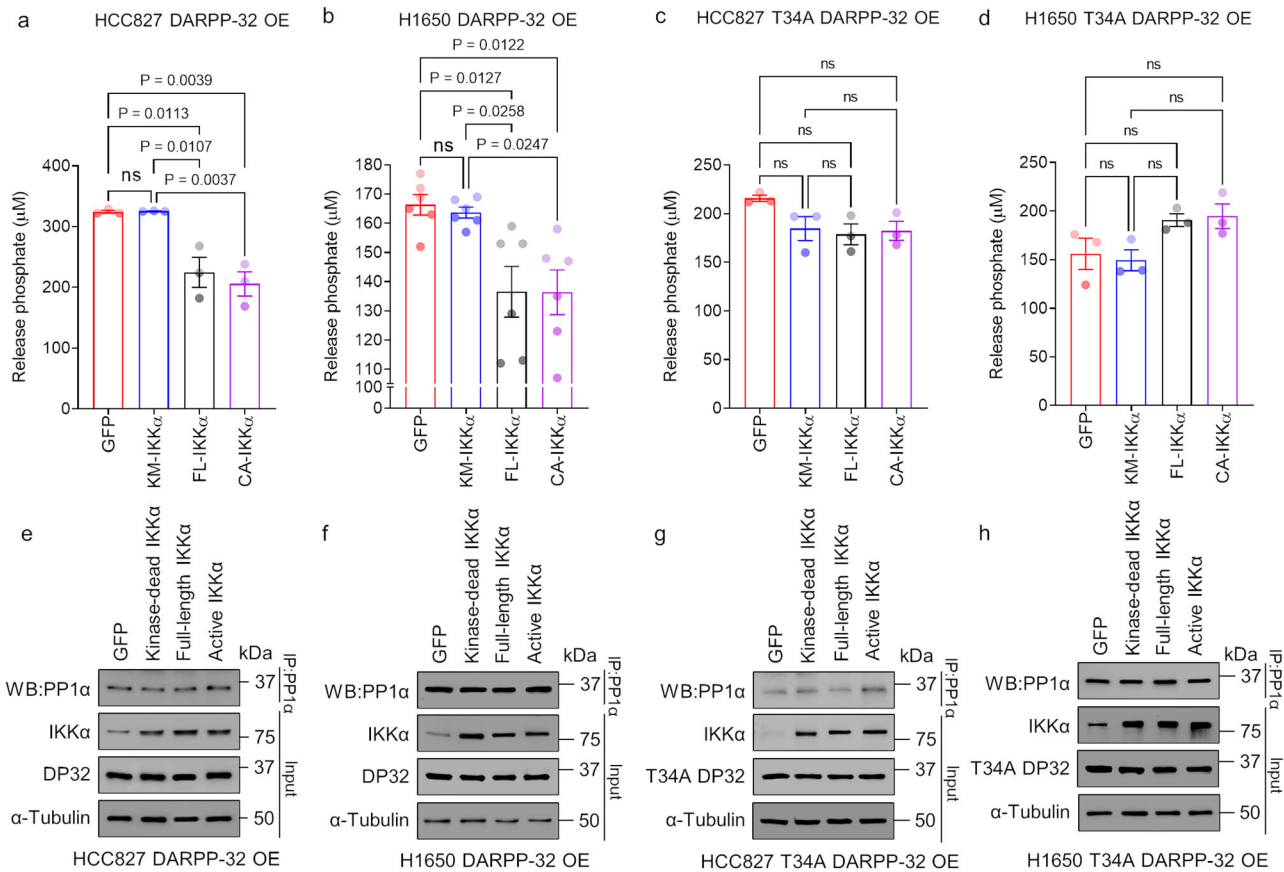


Fig. 4 Overexpression of IKK α inhibits phosphatase activity of PP1 α . **a–d** Human NSCLC HCC827 (**a**, **c**) and H1650 (**b**, **d**) cells transduced with retrovirus designed to overexpress either wild-type (**a**, **b**) or mutant (T34A) DARPP-32 (**c**, **d**) were transfected with GFP (control), kinase-dead (KD), full-length (FL), and constitutively active (CA) IKK α cDNAs were lysed using 1 \times RIPA buffer supplemented with protease inhibitors only. Equal amounts of proteins (500 ng) were immunoprecipitated using anti-PP1 α antibodies. Immunoprecipitated cell lysates were subjected to *in vitro* phosphatase assays following incubation with either PP1 α substrate or histone H1 peptide (control). Released phosphates in each reaction tube were determined by using a phosphate detection reagent. *In vitro* phosphatase experiments were repeated three times independently. Bar graphs represent the mean \pm SEM of the three repeats, with each circle in a bar representing an independent experiment. A value of $P \leq 0.05$ was considered significant, ns not significant, one-way ANOVA followed by Dunnett's test. **e–h** Immunoprecipitated HCC827 (**e**, **g**) and H1650 (**f**, **h**) cell lysates separated with 4–20% SDS-PAGE were subjected to western blotting using anti-PP1 α antibodies. Input cell lysates were blotted with antibodies against IKK α , DARPP-32, and α -tubulin (loading control).

promotes lung cancer growth through studies modulating DARPP-32 expression in human lung adenocarcinoma cells that were orthotopically xenografted into SCID mice²⁵. To confirm the role of PP1 α in the regulation of tumor cell growth, we performed anchorage-independent soft agar growth assays in calyculin A-pretreated HCC827, PC9, and H1650 cells. Results from immunoblotting experiments show an increase in phosphorylated PP1 α (i.e., inactive) and phosphorylated ERK (i.e., activated) expression after 15 min of calyculin A treatment with a slight increase in cell death, as suggested by the detection of a small amount of cleaved PARP-I at 15 min (Fig. 6a). We observed that pharmacologic inhibition of PP1 α in HCC827, PC9, and H1650 human NSCLC cells increased the number of colonies grown on soft agar, suggesting that reduced PP1 α activity promotes anchorage-independent lung cancer cell growth (Fig. 6b, c). We then tested whether IKK α ablation reduces lung tumor growth in an orthotopic xenograft mouse model. Briefly, luciferase-labeled human HCC827 NSCLC cells were injected into the left thorax of anesthetized SCID mice. After the establishment of the lung tumor, mice were imaged for bioluminescence signals weekly over the course of 7 weeks. Mice challenged with IKK α -ablated HCC827 cells showed less lung tumor growth than mice administered cells transduced with control LacZ shRNA (Fig. 7a, b). Immunoblotting experiments demonstrated a reduction in the expression of

phosphorylated PP1 α (i.e., inactive) and phosphorylated ERK (i.e., activated) in lung tumor tissue lysates harvested from mice challenged with IKK α -ablated HCC827 lung cancer cells relative to lysates harvested from mice that were administered control LacZ shRNA-transduced HCC827 cells (Fig. 7c). We stained mouse lung tumor tissues with hematoxylin and eosin (H&E), and we observed a necrotic core within tumors derived from the mice challenged with stable IKK α -depleted HCC827 cells, whereas lung cancer tissues harvested from mice that received LacZ shRNA-transduced HCC827 cells had little to no necrosis (Fig. 7d). This finding helps explain the tumor growth retardation observed in mice challenged with stable IKK α -depleted HCC827 cells relative to controls. Taken together, our *in vitro* cellular studies and *in vivo* mouse data suggest that IKK α protein drives lung oncogenic tumor growth, and ablation of IKK α expression reduces lung cancer growth.

DISCUSSION

Here, we show that the kinase function of IKK α phosphorylates full-length DARPP-32 protein at the Thr-34 position, which leads to the inactivation of PP1 and subsequent activation of ERK signaling to promote lung tumor growth. The IKK complex, consisting either of IKK α , β , and γ kinases (canonical) or IKK α homodimers (noncanonical), has been studied in the context of inflammation

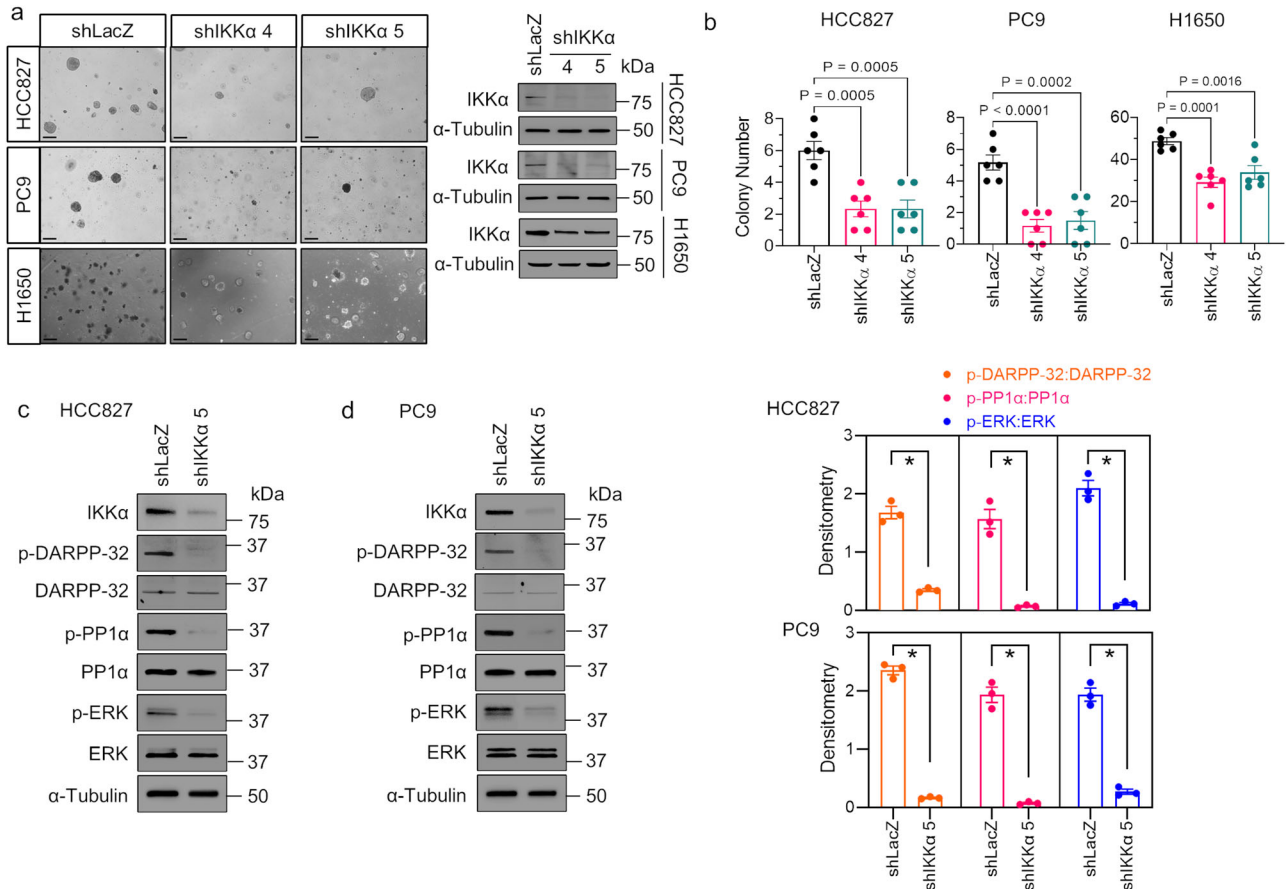


Fig. 5 Knockdown of IKK α protein expression blocks anchorage-independent NSCLC cell growth. **a** Representative images of HCC827, PC9, and H1650 cells transduced with lentivirus encoding either LacZ shRNA or IKK α shRNAs forming colonies on soft-agar cell culture dishes 1 to 2 weeks after plating. **b** Human NSCLC HCC827, PC9, and H1650 cells transduced with lentivirus designed to silence LacZ (control) or IKK α protein expression were subjected to soft-agar colony formation assays to determine anchorage-independent cell growth. ImageJ was used to count colonies on the cell culture dishes after 1 to 2 weeks of incubation, and the number of counted colonies was plotted. Each circle on a graph represents an independent experiment. Soft-agar colony formation experiments were repeated at least six times. Error bars indicate SEM ($n = 6$). Scale bar 200 μm . A value of $P \leq 0.05$ was considered significant, one-way ANOVA followed by Dunnett's test. **c, d** Lysates from HCC827 (**c**) and PC9 (**d**) cells transduced with either LacZ shRNA or IKK α shRNA were subjected to immunoblotting with primary antibodies against IKK α , phosphorylated DARPP-32 (Thr-34), total DARPP-32, phosphorylated PP1 α (Thr320), total PP1 α , phosphorylated ERK (Thr202/Tyr204), total ERK, and α -tubulin (loading control). Bar graphs at the right show values obtained from the densitometric quantification of the results from three western blotting experiments. * $P < 0.05$; Two-tailed unpaired t -test.

and innate immunity as a regulator of interferon regulatory factors and NF- κ B signaling^{42–44}. Recently, it has been appreciated that IKK α and related kinases also phosphorylate proteins involved in controlling biological processes, including cell growth, metabolism, apoptosis, cell cycle, cell migration, and invasion, independent of NF- κ B-regulated cell signaling pathways^{43,45,46}. Overexpression of constitutively active IKK α influences the proliferation of mammary epithelium through regulation of RANK signaling in a genetically engineered mouse model⁴⁷; thus, it is expected that aberrant IKK α expression promotes breast tumorigenesis. Indeed, Bennett et al. reported that overexpression of cytosolic IKK α protein is associated with reduced time to recurrence and worsened disease-free survival in estrogen receptor-positive breast cancer patients⁴⁸. Additionally, the role of IKK α in promoting breast cancer growth in the presence of anti-estrogen therapy via activation of the Notch pathway has been well studied and provides a mechanism for hormone therapy resistance in an NF- κ B-independent manner⁴⁹. Recently, Dan and colleagues reported that IKK α protein activates the AKT cell signaling pathway by phosphorylating the mTOR complex 2 in cervical, prostate, lung, and pancreatic cell lines, establishing the oncogenic role of IKK α protein in promoting tumor growth⁵⁰.

Additionally, transcripts of *CHUK* (IKK α), but not *IKKB* (IKK β), are overexpressed in lung adenocarcinoma tissues compared with normal lung tissues¹⁹. A previous study by our group has shown that NSCLC patients with elevated IKK α expression have significantly reduced overall survival than those with low IKK α expression and that IKK α regulates NSCLC cell migration by forming a complex with DARPP-32 to influence the noncanonical NF- κ B cell signaling pathway²⁵. Here, we propose an alternative mechanism in which activated IKK α protein promotes NSCLC growth through a DARPP-32/PP1 α cell signaling cascade in an NF- κ B-independent manner.

DARPP-32 protein, encoded by the *PPP1R1B* gene, has been well studied in the nervous system to understand the complexity of signal transduction in neurons, especially striatal projection neurons⁵¹. The function of DARPP-32 in amplifying responses to many external stimuli is tightly regulated by its phosphorylation on multiple sites by different protein kinases. Notably, DARPP-32 phosphorylation at Thr-34 by PKA in response to extracellular signals has been shown to inhibit PP1 function in neurons^{23,51}. Similarly, in the context of cancer, PKA has been shown to phosphorylate DARPP-32 at Thr-34 in response to Wnt-5a-mediated stimulation of cAMP³⁹. It is well-established that

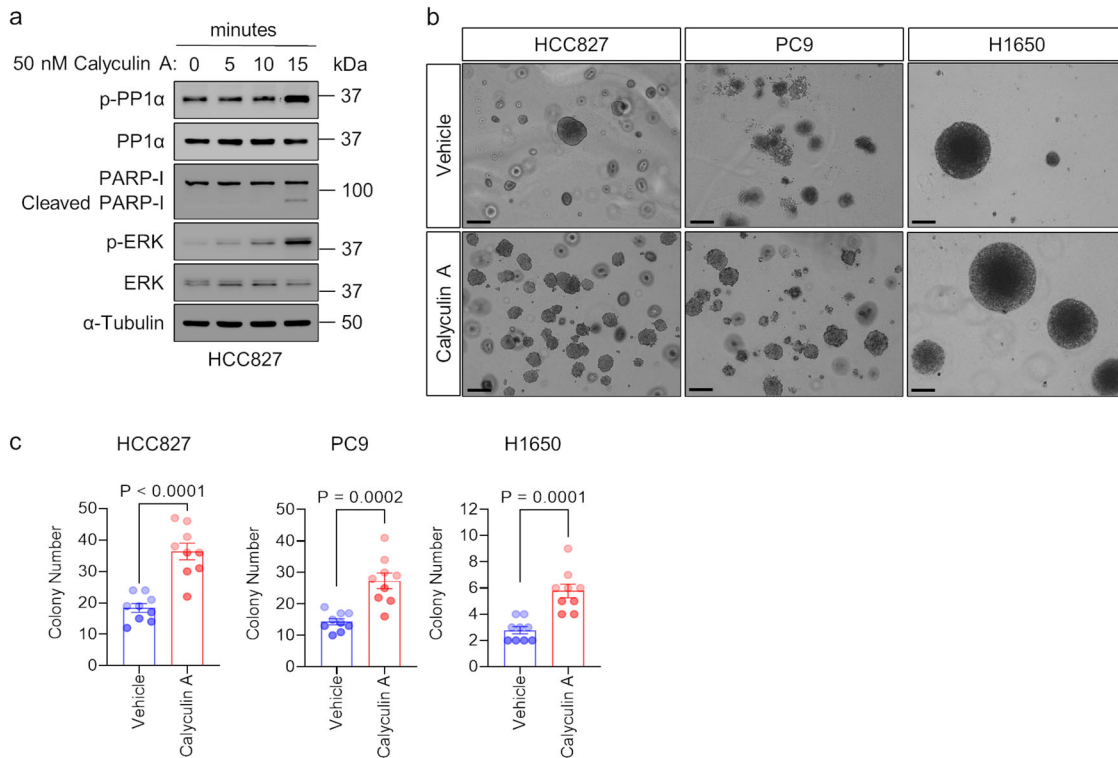


Fig. 6 Inhibition of PP1 phosphatase activity promotes anchorage-independent lung cancer cell growth. **a** Human lung cancer HCC827 cells treated with calyculin A (50 nM) for the indicated times were lysed using 1 \times RIPA buffer supplemented with protease and phosphatase inhibitors. An equal amount of protein was separated with 4–20% SDS-PAGE and transferred to polyvinylidene difluoride membranes. Antibody-reactive protein bands were visualized after overnight incubation of primary antibodies against phosphorylated PP1 α (Thr320), total PP1 α , PARP-I, phosphorylated ERK (Thr202/Tyr204), total ERK, and α -tubulin (loading control). **b** Human NSCLC HCC827, PC9, and H1650 cells were incubated with vehicle (DMSO) or calyculin A (50 nM) for 15 min prior to plating. Representative images indicate cell colonies grown on the soft-agar cell culture dishes after 2 weeks of incubation. Scale bar 200 μ m. **c** Bar graphs show the average count of cell colonies observed after 2 weeks of incubation. Bar graphs indicate mean \pm SEM ($n = 9$). A value of $P \leq 0.05$ was considered significant, two-tailed unpaired t -test.

cAMP-induced PKA activation leads to DARPP-32 phosphorylation at Thr-34, which results in the inhibition of PP1 activity. However, kinases do not regulate t-DARPP through phosphorylation of Thr-34 because the t-DARPP protein isoform lacks the first 36 amino acids that are present in the full-length DARPP-32 protein, including Thr-34.

DARPP-32 and t-DARPP promote non-small cell lung cancer growth through IKK α -dependent activation of noncanonical NF- κ B2 signaling based on our previous findings showing DARPP-32 and t-DARPP each have oncogenic properties in lung cancer cells, including regulation of cell survival and migration²⁵. We also showed in NSCLC^{25,34} and small cell lung cancer²⁶ that overexpression of DARPP-32 or t-DARPP leads to increased ERK1/2 activation, whereas shRNA-mediated knockdown of DARPP-32 isoforms results in reduced ERK1/2 phosphorylation. Our findings presented here suggest that overexpression of kinase-active IKK α protein positively regulates the ERK pathway through the DARPP-32/PP1 α axis. Specifically, we observed greater inactivation (i.e., phosphorylation) of PP1 α proteins in NSCLC cells stably overexpressing exogenous DARPP-32 upon transient expression of constitutively active IKK α cDNA plasmids relative to wild-type or kinase-dead IKK α control expression vectors. Conversely, NSCLC cells stably overexpressing full-length DARPP-32 containing a T34A mutation that were transiently transfected with constitutively active IKK α cDNA did not exhibit increased phosphorylation (i.e., inactivation) of PP1 α relative to the aforementioned controls. Thus, our collective findings suggest that IKK α phosphorylates DARPP-32 at the Thr-34 residue, which causes DARPP-32 to inactivate PP1 α via phosphorylation, leading to activation

(i.e., greater phosphorylation) of ERK1/2. Because the N-terminally truncated t-DARPP protein isoform lacks the Thr-34 residue, IKK α does not regulate t-DARPP through the phosphorylation of Thr-34. Upregulation of t-DARPP leads to increased activation of ERK signaling^{25,26,34}; however, the molecular mechanism(s) by which t-DARPP activates ERK signaling in lung cancer are not well understood. The strong presence of t-DARPP protein phosphorylated at Thr-39 (equivalent to full-length DARPP-32 Thr-75) in our assays warrants future investigation to identify the molecular mechanism(s) of t-DARPP regulation by upstream kinases in NSCLC cells. t-DARPP may be phosphorylated by IKK α and/or other kinases at sites other than Thr-39 in t-DARPP (i.e., Thr-75 in full-length DARPP-32). An in vitro kinase experiment using radiolabeled ATP may shed light on whether IKK α phosphorylates t-DARPP protein at other sites.

Recently, it was shown that breast cancer patients with elevated DARPP-32 expression but low PP1 expression have worse overall survival than those with low expression of DARPP-32⁵², suggesting a strong inverse correlation between PP1 and DARPP-32 proteins in patient outcome. This supports the notion that DARPP-32-mediated inactivation of PP1 functions via phosphorylation leads to increased activation of kinases involved in oncogenic signaling pathways. Moreover, PKA protein expression in breast tumor tissues shows a strong correlation with DARPP-32 and PP1 protein expression, warranting further investigation to understand the molecular mechanism in regulating breast tumorigenesis⁵². In a separate study, Hansen et al. reported that PKA protein activated by Wnt-5a ligands regulates breast cancer cell migration by phosphorylating DARPP-32 at Thr-34 in a PP1/CREB-dependent

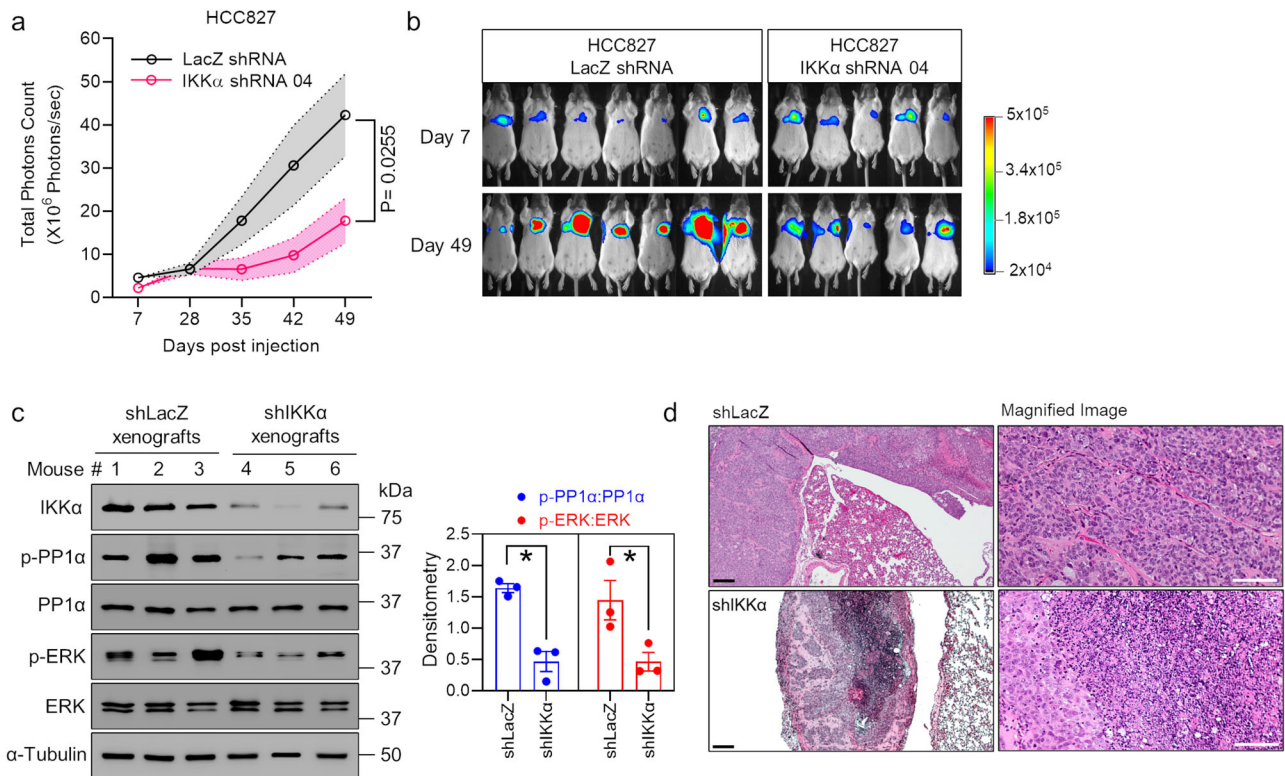


Fig. 7 Depletion of IKK α inhibits lung tumor cell growth and proliferation in vivo. **a** Luciferase-labeled IKK α -depleted human HCC827 cells were orthotopically injected into the left thorax of SCID mice and imaged for luminescence on the indicated days. Total luminescence intensity (photon count) was calculated using molecular imaging software and plotted as a line graph. Error bars are shown as dotted lines indicating SEM. A value of $P \leq 0.05$ was considered significant, two-way ANOVA followed by Sidak's test. **b** Images of anesthetized mice were captured to detect luminescence signals on the indicated days. **c** Tumor tissue lysates obtained from either LacZ shRNA- or IKK α shRNA-transduced human HCC827 cells-derived xenografts were subjected to immunoblotting using primary antibodies against IKK α , phosphorylated PP1 α (Thr320), total PP1 α , phosphorylated ERK (Thr202/Tyr204), total ERK, and α -tubulin (loading control). Bar graphs show densitometric quantification values of the results from three western blotting experiments. * $P < 0.05$; Two-tailed unpaired t-test. **d** Overall morphological evaluation was performed on formalin-fixed, paraffin-embedded lung tissues ($n = 5$ mice per group) obtained from human HCC827 cells-derived lung tumor xenograft mice model using hematoxylin and eosin (H&E) dye. Scale bar 50 μ m.

manner³⁹. In line with this observation, our prior report suggests DARPP-32 promotes NSCLC cell migration²⁵, and our current study provides strong evidence that NSCLC cell growth is regulated by the IKK α /DARPP-32/PP1/ERK cell signaling pathway. Overexpression of t-DARPP has been shown to confer resistance to trastuzumab, a HER2-targeted monoclonal antibody, via activation of PKA and PI3K/AKT cell signaling in HER2⁺ breast cancer cells^{53,54}. A molecular mechanism has recently been identified in which t-DARPP phosphorylated by CDK-1 and -5 activates PKA kinase function by forming a direct complex with PKA regulatory subunits in breast cancer cells overexpressing t-DARPP^{32,33}.

The catalytic subunit of PP1, a major protein phosphatase in human cells composed of α , β , and γ subunits, regulates critical cellular processes, including cell cycle progression, apoptosis, and metabolism by catalyzing dephosphorylation of a wide range of proteins⁵⁵. The role of PP1 as a tumor suppressor or oncogene depends on the type of cancer, the stage of cancer progression, and the regulatory proteins that interact with PP1. The pathways are further complicated because both oncogenes and tumor suppressor proteins are known substrates of PP1, and dephosphorylation events can activate or downregulate downstream cell signaling pathways⁵⁶. Therefore, detailed mechanistic insight is needed to understand the role of PP1 in lung cancer. The complex of PP1 with the leucine-rich repeat protein SHOC2 promotes tumor growth in a subset of KRAS-mutant NSCLC cell lines by dephosphorylating a critical inhibitory site on RAF kinases, resulting in RAF-ERK pathway activation. Moreover, genetic inhibition of SHOC2 suppresses tumor development in

autochthonous murine *Kras*-driven lung cancer models⁵⁷. In contrast, activated PP1, upon forming a complex with protein 4.1N, a neuronal homolog of the erythrocyte membrane cytoskeletal protein 4.1, inhibits lung tumor progression by suppressing the JNK cell signaling pathway⁵⁸. Our results suggest that PP1-mediated dephosphorylation of ERK is inhibited by the DARPP-32/PP1 complex, which in turn promotes lung tumor growth by increasing ERK activity. Increased activation of ERK is associated with elevated oncogenic potential due to the central position of ERK downstream of several oncogenic growth signaling pathways.

Manipulation of PP1 activity has long been considered a potential approach to treating cancer because of the involvement of PP1 in several cancer-related cellular processes. The small-molecule inhibitors calyculin A and okadaic acid have been used to mitigate PP1 and PP2A activity, thereby impairing the progression of hormone therapy-resistant prostate cancer by stimulating cell death⁵⁹. However, PP1 small-molecule inhibitors have unwanted cellular toxicity because PP1 is involved in a broad range of cellular processes. Moreover, the homology of the active sites among different phosphatases contributes to the limited efficacy of these inhibitors in treating cancer. Therefore, targeting PP1 complexes, instead of focusing on the catalytic sites of PP1, is a promising solution to suppress sustained growth and survival in cancer.

Recent findings of interesting, novel phosphorylation substrates of IKK family kinases, including DARPP-32 in this study, expand current knowledge of critical biological and disease-related

mechanisms. To comprehensively understand the function of these pleiotropic kinases, further experiments are needed to assess the roles of IKK family members in regulating phosphorylation-dependent substrates in different settings and diseases. In this regard, it will be important to see whether DARPP-32 phosphorylation is regulated by IKK α protein in the presence of anticancer agents routinely used in the clinic to treat lung cancers. Another critical question—which upstream kinases regulate IKK α activation—warrants further investigation because EGFR and KRAS are highly mutated in lung cancer patients⁶⁰. Importantly, the results we report here were primarily based on studies using three EGFR-mutated NSCLC cell lines, H1650, HCC827, and PC9. KRAS is not mutated in any of these three cell lines, so testing whether ERK signaling is activated via DARPP-32-mediated inhibition of PP1 activity in the context of KRAS-mutated NSCLC warrants future investigation. Targeting IKK and IKK-related kinases with the small-molecule IKK inhibitors SAR-113945 and MLN-0415 has shown encouraging results in preclinical studies, although they failed to meet the primary endpoints of a phase 2 clinical trial and the safety profile of a phase 1 clinical trial, respectively⁶¹. Because NF- κ B functions in many different systems, targeting IKK α and IKK-related kinases to treat disease, including cancers, can result in unpredictable adverse events. Therefore, the development of more selective, isoform-specific, non-ATP-competitive inhibitors against IKK family kinases to use in combination therapies and/or as part of a targeted delivery approach is required, particularly in cancers that aberrantly express IKK α protein.

METHODS

Cell lines and inhibitors

Human NSCLC cell lines A549 (KRAS^{G12S} and STK11^{mut}) and H1650 (EGFR^{ΔE746-A750} and TP53^{deletion}), as well as a transformed human embryonic kidney epithelial cell line, HEK-293T, were purchased from the American Type Culture Collection. The epidermal growth factor receptor (EGFR)-mutated human NSCLC cell lines HCC827 (EGFR^{ΔE746-A750} and TP53^{deletion}), PC9 (EGFR^{AMP}, EGFR^{ΔE746-A750}, TP53^{R248Q}, and CDKN2A^{G67V}) and H1975 (EGFR^{L858R+T790M} and TP53^{R273H}) were kindly provided by Dr. Pasi A. Jänne at the Dana-Farber Cancer Institute⁶², Dr. Aaron N. Hata at Massachusetts General Hospital⁶³, and Dr. Anthony C. Faber at Virginia Commonwealth University⁶⁴, respectively. Dulbecco's modified Eagle's medium (DMEM; Corning, Cat no. 10-013-CV) supplemented with 10% fetal bovine serum (FBS; Millipore, Cat no. TMS-013-B) was used to grow HEK-293T cells. Human NSCLC cell lines A549, H1650, HCC827, PC9, and H1975 were maintained in Roswell Park Memorial Institute (RPMI)-1640 medium (Corning, Cat no. 10-040-CV) supplemented with 10% FBS (Millipore), 1% penicillin/streptomycin antibiotics (Corning, Cat no. 30-002-CI), and 25 μ g/mL plasmocin prophylactic (Invivogen, Cat no. ant-mpp). All cell lines were routinely authenticated via morphologic inspection and tested negative for mycoplasma contamination. A serine/threonine protein phosphatase inhibitor, calyculin A, purchased from Cell Signaling Technology (CST, Cat no. 9902), was used to mitigate PP1 α function.

Generation of stable cell lines

Human full-length DARPP-32, t-DARPP, and mutant DARPP-32 (T34A) cDNAs cloned into the pCDNA3.1 vector were kindly provided by Dr. Wael El-Rifai at the University of Miami Health System⁶⁵. The FLAG-tagged coding sequence of DARPP-32, t-DARPP, and DARPP-32 T34A were subcloned into a retroviral (pMMP) vector. Retrovirus containing FLAG-tagged full-length DARPP-32, t-DARPP, and mutant DARPP-32 cDNAs were prepared by following a previously described procedure^{25,34}. Briefly, 5 μ g of the cDNA plasmids (pMMP-DARPP-32, pMMP-t-DARPP, pMMP-T34A DARPP-32, or corresponding control pMMP-LacZ), 1.5 μ g of

pMD.MLV.gag.pol packaging plasmid DNA, and 0.5 μ g of pMD.2G envelope plasmid DNA were used to transfect 10 cm dishes of 293 T cells after mixing with 300 μ l of EC buffer (Qiagen), 32 μ l of Enhancer (Qiagen), and 30 μ l of Effectene (Qiagen, Cat no. 301425). Media was replaced 16 h post-transfection. The supernatant containing retroviral particles was collected at 48 and 72 h post-transfection. Viral supernatant was filtered through 0.45-micron sterile filters, concentrated via Retro-X Concentrator (Clontech, Cat no. 631455), resuspended in 1 ml RPMI-1640 media, aliquoted, and stored at -80°C until used. NSCLC cells seeded at a density of 3×10^5 cells per 10-cm cell culture dish were transduced with 1 mL retrovirus diluted in 5 mL fresh medium supplemented with 10 μ g/mL polybrene solution (Millipore, Cat no. TR-1003-G). Cells were used for subsequent experiments 48 h after transduction. The pMMP plasmid, its corresponding control pMMP-LacZ vector, the pMD.MLV.gag.pol packaging plasmid, and the pMD.2G envelope plasmid were kindly provided by Dr. Debabrata Mukhopadhyay at Mayo Clinic, Jacksonville, FL.

Lentiviral vectors (pLKO.1) designed to silence IKK α (shIKK α #4: GCAAATGAGGAACAGGGCAAT; shIKK α #5: GCGTGCCATTGATCTA TATAA) and LacZ as a control (shLacZ: CCAACGTGACCTATCC CATTAA) were purchased from Sigma. Briefly, 5 μ g of the lentiviral plasmids, along with their corresponding packaging plasmids (similar to the retroviral transfection method), were transfected into human 293 T cells using the Effectene transfection reagent (Qiagen) as described above. Fresh complete growth medium was added to cell culture plates at 16 h post-transfection. Viral supernatant was collected at 48 and 72 h post-transfection, filtered through 0.45-micron sterile filters, concentrated using Lenti-X concentrators (Clontech, Cat no. 631231), and used immediately to transduce HCC827 and PC9 lung cancer cell lines, as reported previously⁶⁶. Transduced cells were incubated in a medium containing puromycin (Sigma, Cat no. P8833) for 72 h to select stable IKK α knockdown cells.

Retroviruses containing the luciferase gene were prepared in 293 T cells as described previously²⁶. Briefly, the retrovirus-based firefly luciferase expression vector (MSCV IRES Luciferase) along with packaging plasmid (gag/pol) and envelope expressing plasmid (pCMV-VSV-G) from Addgene were co-transfected into 293 T cells. The MSCV IRES Luciferase plasmid, gag/pol vector, and pCMV-VSV-G plasmid were gifts from Scott Lowe (Addgene plasmid #18760), Tannishtha Reya (Addgene plasmid #14887)⁶⁷, and Bob Weinberg (Addgene plasmid #8454)⁶⁸, respectively. Retroviral particles were collected after 48 and 72 h of transfection, filtered through 0.45-micron sterile filters, concentrated via Retro-X Concentrator (Clontech, Cat no. 631455), resuspended in complete RPMI-1640 medium, aliquoted, and stored at -80°C until used.

To generate luciferase-labeled stable human NSCLC cells, 0.6×10^6 cells were plated in 6 cm cell culture dishes and incubated at 37°C overnight. On the next day, human NSCLC cells were transduced by adding a mixture of 3 ml complete cell culture growth media, 3.5 μ l Polybrene (10 μ g/ml; Millipore), and 500 μ l concentrated virus. Cells were selected using 500 μ g/ml of Hygromycin (Sigma, Cat no. H7772) every 2–3 days until the corresponding plates of Hygromycin-treated control (i.e., not transduced) cells had died. Luciferase-labeled stable human NSCLC cells were used to determine tumor growth in orthotopic murine models.

Antibodies

Primary antibodies (1 μ g/ μ l) identifying two different phosphorylated sites on DARPP-32 (T34: cat no. 12438; dilution 1:1000; and T75: cat no. 2301; dilution 1:1000), phosphorylated PP1 α (T320; cat no. 2581; dilution 1:1000), IKK α (cat no. 2682; dilution 1:1000), phosphorylated p44/42 MAPK (T202/Y204; cat no. 4370; dilution 1:1000), and total p44/42 MAPK (cat no. 4695; dilution 1:1000) were purchased from CST. Antibodies (200 μ g/ml) against DARPP-32 (cat no. sc-398360; dilution 1:200), PP1 (cat no. sc-7482; dilution

1:100), and α -tubulin (cat no. sc-5286; dilution 1:500) were obtained from Santa Cruz Biotechnology. Horseradish peroxidase (HRP)-conjugated secondary antibodies against the heavy chains of anti-rabbit (cat no.: 7074; dilution 1:5000) and anti-mouse (cat no.: 7076; dilution 1:5000) IgG were purchased from CST.

Plasmids

Expression vectors of full-length (#15467) and kinase-dead (#15468) mouse IKK α , as well as constitutively kinase-active (#64608) human IKK α , were purchased from Addgene. Briefly, the investigators constructed a full-length IKK α in-frame with DNA encoding an N-terminal FLAG epitope in pCR-3 vectors⁶⁹. Kinase-dead IKK α (K44A) was generated from full-length IKK α expression plasmids by using a site-directed mutagenesis kit⁶⁹. Expression vectors for V5 epitope-tagged constitutively kinase-active IKK α (S176E, S180E) were constructed in destination/expression vector pcw107 via the Gateway cloning system⁷⁰. When overexpressed, constitutively kinase-active IKK α (S176E, S180E) plasmid constitutively activates the NF- κ B pathway in a ligand-independent manner. Expression plasmids (pCMV) encoding GFP used as transfection controls were kindly shared by Dr. Georgiy Aslanidi at The Hormel Institute, University of Minnesota.

Immunoblotting

Radioimmunoprecipitation assay (RIPA; 0.5 M Tris-HCl, pH 7.4; 1.5 M NaCl, 2.5% deoxycholic acid, 10% NP-40, 10 mM EDTA) buffer (Millipore, Cat no. 20-188) supplemented with protease inhibitor cocktail (Roche, Cat no. 5892970001) and phosphatase inhibitors (Millipore, Cat no. 524629) were used to lyse human NSCLC cells on ice. Protein was quantified using Quick startTM Bradford 1X dye reagent (Bio-Rad, Cat no. 5000205) using a standard curve created with different concentrations of BSA. Equal amounts of cell lysates were separated via 4–20% gradient SDS-PAGE (Bio-Rad; Cat no. 4568094) and transferred to polyvinylidene difluoride membranes (Millipore, Cat no. IPVH00010). Prior to primary antibody incubation, membranes were cut into pieces based on the location of the pre-stained blue molecular weight marker (Bio-Rad, Cat no. 1610393) such that multiple membranes derived from the same immunoblotting gel could be stained with different antibodies detecting differently sized proteins. These membranes were then incubated in Tris-buffered saline (50 mM Tris-Cl, pH 7.6; 150 mM NaCl; GrowCells, Cat no. 75800-902) containing 5% bovine serum albumin (Sigma, Cat no. A7906) at room temperature for 1 h. Incubation of diluted primary and secondary antibodies was carried out overnight at 4 °C and for 2 h at room temperature, respectively. Chemiluminescence substrate (Thermo Fisher Scientific, Cat no. PI34580) was used to detect antibody-reactive protein bands in the membranes, and signals were captured electronically using an ImageQuantTM LAS 4000 instrument (GE Healthcare). To detect protein bands of similar molecular weight, we performed multiple concurrent immunoblotting experiments using equal aliquots of the same cell lysates run on different gels and/or membranes. All immunoblots derived from concurrent immunoblotting experiments were processed in parallel. Images of uncropped and unprocessed scans of the immunoblots are included in Supplementary Figs. 2–21.

Purification of DARPP-32 isoforms

Human lung adenocarcinoma A549, HCC827, PC9, and H1975 cells stably overexpressing FLAG-tagged DARPP-32 or t-DARPP proteins were grown to 95–100% confluency in 150-mm cell culture plates. Cells were lysed on ice using 1 ml of 1 × lysis buffer (50 mM Tris-HCl, pH 7.4, with 150 mM NaCl, 1 mM EDTA, and 1% Triton X-100) supplemented with protease inhibitor cocktail (Roche). For each cell line, lysates were pooled from five plates and incubated

overnight with anti-FLAG M2 agarose (Sigma, Cat no. A2220) on a rotating platform at 4 °C. Positively selected FLAG fusion proteins were collected by centrifugation at 1000×g for 5 min and washed with TBS. Protein elution was carried out under native conditions by incubation with 200 μ l 3X FLAG peptide (GLP BIO, Cat no. GP10149F5) at a concentration of 150 ng/ μ l in TBS for 30 min at 4 °C and then collected following centrifugation for 30 s at 5000×g. The elution process was repeated twice and a total of 400 μ l eluted FLAG fusion protein was concentrated to 40 μ l using 0.5 mL Ultracel[®] 30 K membrane (Millipore, Cat no. UFC503008). Protein was quantified using Quick startTM Bradford 1X dye reagent (Bio-Rad, Cat no. 5000205) using a standard curve created with different concentrations of BSA. Eluted proteins were run on 4–20% polyacrylamide gels in denatured conditions and visualized following Coomassie blue (Bio-Rad, Cat no. 1610786) staining.

In vitro kinase assay

Human DARPP-32 isoforms purified from NSCLC cells were incubated with kinase-activated human IKK α protein (SignalChem, Cat no. C51-10G-10) in 50 μ l reaction volume for in vitro kinase assays by following previously described methods⁷¹. Briefly, 3 μ g purified DARPP-32 isoforms as well as 5 μ l ATP (New England Biolabs, Cat no. N0440) in kinase dilution buffer III (5 mM MOPS, pH 7.2; 2.5 mM β -glycerol-phosphate, 5 mM MgCl₂, 1 mM EGTA, 0.4 mM EDTA, 50 ng/ μ l BSA; SignalChem, Cat no. K23-09-05) were incubated with 1 μ g commercially available human IKK α protein (SignalChem) for 30 min at 30 °C, then at 95 °C for 5 min, in which 1 × Laemmli sample buffer (Bio-Rad, Cat no. 1610747) supplemented with 10% β -mercaptoethanol (Bio-Rad, Cat no. 1610710) was added to stop the kinase reaction. Phosphorylation of DARPP-32 by kinase-activated human IKK α protein was validated via immunoblotting using monoclonal primary antibodies against phosphorylated DARPP-32 (T34 and T75, CST).

Transient transfection

Human NSCLC cell lines, HCC827 or H1650, were plated in 6-well cell culture plates at a concentration of 2×10^5 cells per well. Cells were washed with PBS (Corning, Cat no. 1610747) on the following day prior to transfection, and a complete RPMI-1640 medium (Corning) was added to each well. Based on the protocols from the manufacturer, 2.5 μ g of plasmid DNA and 5 μ l P3000 reagent (Invitrogen, Cat no. L3000001) diluted in OPTI-MEM medium (Gibco, Cat no. 31985062) were incubated with 10 μ l Lipofectamine-3000 transfection reagent (Invitrogen, Cat no. L3000001) for 15 min at room temperature. The DNA:Lipofectamine mixture was then added to each well in a dropwise manner and incubated for 48 h.

Immunoprecipitation

Human NSCLC cell lines at a concentration of 3×10^6 cells per 100-mm cell culture dish transiently transfected with either control GFP or one of three different IKK α plasmids were lysed in RIPA buffer (Millipore) supplemented with protease inhibitors (Roche). The concentration of harvested cell lysates was measured by using the Bradford reagent (Bio-Rad, Cat no. 5000205). Anti-PP1 α antibody (2 μ g; SCBT, Cat no. sc-7482) was added to the supplied spin column (Catch and Release Immunoprecipitation Kit; cat no. 17-500; Millipore) along with the cell lysates (500 μ g) to immunoprecipitate the proteins following the manufacturer's protocol. The eluted proteins in their native form were subsequently used to perform the in vitro phosphatase assay.

In vitro phosphatase assay

The in vitro phosphatase assay was performed in accordance with the manufacturer's protocol. Briefly, 5 μ l PP1 α substrates (GRPRTS[p]

SFAEG; SignalChem, Cat no. P50-58) or 5 μ l control histone H1 peptides (GGGPATP-KKAKKL-COOH; SignalChem, Cat no. H10-58) diluted in phosphatase dilution buffer II (50 mM Imidazole, pH 7.2, 0.2% 2-mercaptoethanol, 65 ng/ μ l BSA; SignalChem, Cat no. P22-09) was incubated for 15 min at 37 °C with human PP1 α protein in its native form immunoprecipitated from human NSCLC cells at a final volume of 30 μ l. The amount of free phosphate molecules generated by the reaction was colorimetrically quantified with a Phosphate Assay Kit (Abcam, Cat no. ab65622). The amount of released phosphate was determined from a standard curve generated after plotting the absorbance value against increasing known concentrations of free phosphate molecules.

Soft-agar colony formation assay

Five milliliters of complete RPMI-1640 medium (Corning) containing 0.75% melted agar (Sigma, Cat no. A9045) was added to 60-mm cell culture dishes to create a bottom layer. Cells of the human NSCLC lines HCC827, PC9, and H1650 transduced with lentivirus encoding LacZ shRNA (control) or IKK α shRNAs were suspended in complete RPMI-1640 medium containing 0.36% melted agar and were plated on top of the bottom layer at a concentration of 2.5×10^4 cells per dish. After 1 (H1650) to 2 weeks (HCC827 and PC9) of incubation, images of colonies that had grown on the soft-agar cell culture plates were captured using a 4 \times Plan S-Apo 0.16 NA objective on an EVOS FL cell imaging system (Thermo Fisher Scientific). The colonies were counted by using ImageJ software and plotted by using GraphPad Prism 9 software. Similarly, 3×10^4 HCC827, PC9, and 1×10^4 H1650 cells were first incubated with either vehicle (DMSO) or calyculin A (50 nM) for 15 min. Cells were then resuspended in fresh RPMI-1640 medium containing 0.36% melted agar and plated on the soft-agar cell culture plates. After 2 weeks of incubation, images were captured and analyzed using ImageJ software.

In vivo orthotopic lung cancer model

Six- to eight-week-old pathogen-free SCID/NCr mice were purchased from Charles River Laboratories. Mice were allowed one week to acclimate to their surroundings, then bred, maintained under specific-pathogen-free conditions in a temperature-controlled room with alternating 12 h light/dark cycles, and fed a standard diet in accordance with protocols approved by the University of Minnesota Institutional Animal Care and Use Committee. For each mouse, luciferase-labeled human HCC827 lung cancer cells (1×10^6) transduced with either LacZ shRNA (control) or IKK α shRNAs were suspended in 80 μ l PBS and Matrigel (Corning, Cat no. 354248). The cells were then orthotopically injected in the right thoracic cavity of 8- to 12-week-old male and female mice and allowed to establish tumors over 1 week. Luminescence images of mice were taken weekly over 7 weeks using an In Vivo Xtreme xenogen imaging system (Bruker). The luciferase intensity (total photon count) of each mouse was calculated using Bruker molecular imaging software and plotted over time in GraphPad Prism 9 software.

Statistics

Statistically significant differences between multiple groups (greater than 2) were determined by performing a one-way analysis of variance (ANOVA) followed by Dunnett's test. To compare differences between two groups, two-tailed unpaired t-tests were performed. Statistically significant differences in tumor growth over time between the two groups in the mouse experiments were determined with two-way ANOVA followed by Sidak's test. Values of $P \leq 0.05$ were considered significant. Data were expressed as mean \pm SEM of at least three independent experiments.

Reporting summary

Further information on research design is available in the Nature Research Reporting Summary linked to this article.

DATA AVAILABILITY

The authors declare that the data supporting the findings of this study are available within the article and its supplementary information. Any other associated data supporting the findings of this study are available from the corresponding author upon request.

Received: 22 July 2022; Accepted: 8 March 2023;

Published online: 25 March 2023

REFERENCES

- Sung, H. et al. Global cancer statistics 2020: GLOBOCAN estimates of incidence and mortality worldwide for 36 cancers in 185 countries. *CA Cancer J. Clin.* **71**, 209–249 (2021).
- Ferlay, J. et al. Cancer statistics for the year 2020: an overview. *Int. J. Cancer.* <https://doi.org/10.1002/ijc.33588> (2021).
- Travis, W. D. et al. The 2015 World Health Organization classification of lung tumors: impact of genetic, clinical and radiologic advances since the 2004 classification. *J. Thorac. Oncol.* **10**, 1243–1260 (2015).
- Howlader, N. et al. The effect of advances in lung-cancer treatment on population mortality. *N. Engl. J. Med.* **383**, 640–649 (2020).
- Ng, M. et al. Smoking prevalence and cigarette consumption in 187 countries, 1980–2012. *JAMA* **311**, 183–192 (2014).
- Siegel, R. L., Miller, K. D., Fuchs, H. E. & Jemal, A. Cancer statistics, 2022. *CA Cancer J. Clin.* **72**, 7–33 (2022).
- Islami, F. et al. Annual report to the nation on the status of cancer, Part 1: national cancer statistics. *J. Natl Cancer Inst.* **113**, 1648–1669 (2021).
- Thai, A. A., Solomon, B. J., Sequist, L. V., Gainor, J. F. & Heist, R. S. Lung cancer. *Lancet* **398**, 535–554 (2021).
- Senftleben, U. et al. Activation by IKK α of a second, evolutionary conserved, NF- κ B signaling pathway. *Science* **293**, 1495–1499 (2001).
- Hayden, M. S., West, A. P. & Ghosh, S. NF- κ B and the immune response. *Oncogene* **25**, 6758–6780 (2006).
- Ghosh, S. & Karin, M. Missing pieces in the NF- κ B puzzle. *Cell* **109**, S81–S96 (2002).
- Zandi, E., Rothwarf, D. M., Delhase, M., Hayakawa, M. & Karin, M. The I κ B kinase complex (IKK) contains two kinase subunits, IKK α and IKK β , necessary for I κ B phosphorylation and NF- κ B activation. *Cell* **91**, 243–252 (1997).
- Mercurio, F. et al. IKK-1 and IKK-2: cytokine-activated I κ B kinases essential for NF- κ B activation. *Science* **278**, 860–866 (1997).
- Sun, S.-C. The non-canonical NF- κ B pathway in immunity and inflammation. *Nat. Rev. Immunol.* **17**, 545–558 (2017).
- Li, X. & Hu, Y. Attribution of NF- τ B activity to CHUK/IKK α -involved carcinogenesis. *Cancers* **13**, 1411 (2021).
- Zhang, W. et al. A NIK-IKK α module expands ErbB2-induced tumor-initiating cells by stimulating nuclear export of p27/Kip1. *Cancer Cell* **23**, 647–659 (2013).
- Luo, J. L. et al. Nuclear cytokine-activated IKK α controls prostate cancer metastasis by repressing Maspin. *Nature* **446**, 690–694 (2007).
- Page, A. et al. IKK α promotes the progression and metastasis of non-small cell lung cancer independently of its subcellular localization. *Comput. Struct. Biotechnol. J.* **17**, 251–262 (2019).
- Vreka, M. et al. I κ B kinase α is required for development and progression of KRAS-mutant lung adenocarcinoma. *Cancer Res.* **78**, 2939–2951 (2018).
- Song, N. Y. et al. IKK α inactivation promotes Kras-initiated lung adenocarcinoma development through disrupting major redox regulatory pathways. *Proc. Natl Acad. Sci. USA* **115**, E812–E821 (2018).
- Brené, S. et al. Expression of mRNAs encoding ARPP-16/19, ARPP-21, and DARPP-32 in human brain tissue. *J. Neurosci.* **14**, 985–998 (1994).
- Brené, S. et al. Distribution of messenger RNAs for D1 dopamine receptors and DARPP-32 in striatum and cerebral cortex of the cynomolgus monkey: relationship to D1 dopamine receptors. *Neuroscience* **67**, 37–48 (1995).
- Svenningsson, P. et al. DARPP-32: an integrator of neurotransmission. *Annu. Rev. Pharmacol. Toxicol.* **44**, 269–296 (2004).
- Hemmings, H. C. Jr, Greengard, P., Tung, H. Y. & Cohen, P. DARPP-32, a dopamine-regulated neuronal phosphoprotein, is a potent inhibitor of protein phosphatase-1. *Nature* **310**, 503–505 (1984).
- Alam, S. K. et al. DARPP-32 and t-DARPP promote non-small cell lung cancer growth through regulation of IKK α -dependent cell migration. *Commun. Biol.* **1**, 43 (2018).

26. Alam, S. K. et al. ASCL1-regulated DARPP-32 and t-DARPP stimulate small cell lung cancer growth and neuroendocrine tumour cell proliferation. *Br. J. Cancer* **123**, 819–832 (2020).
27. Ebihara, Y. et al. DARPP-32 expression arises after a phase of dysplasia in oesophageal squamous cell carcinoma. *Br. J. Cancer* **91**, 119–123 (2004).
28. El-Rifai, W. et al. Gastric cancers overexpress DARPP-32 and a novel isoform, t-DARPP. *Cancer Res.* **62**, 4061–4064 (2002).
29. Martin, S. G. et al. Dopamine and cAMP-regulated phosphoprotein 32kDa (DARPP-32), protein phosphatase-1 and cyclin-dependent kinase 5 expression in ovarian cancer. *J. Cell Mol. Med.* **24**, 9165–9175 (2020).
30. Tiwari, A. et al. Loss of HIF1A from pancreatic cancer cells increases expression of PPP1R1B and degradation of p53 to promote invasion and metastasis. *Gastroenterology* **159**, 1882–1897.e1885 (2020).
31. Christenson, J. L. & Kane, S. E. Darpp-32 and t-Darpp are differentially expressed in normal and malignant mouse mammary tissue. *Mol. Cancer* **13**, 192 (2014).
32. Theile, D., Geng, S., Denny, E. C., Momand, J. & Kane, S. E. t-Darpp stimulates protein kinase A activity by forming a complex with its RI regulatory subunit. *Cell Signal* **40**, 53–61 (2017).
33. Momand, J. et al. t-Darpp is an elongated monomer that binds calcium and is phosphorylated by cyclin-dependent kinases 1 and 5. *FEBS Open Biol.* **7**, 1328–1337 (2017).
34. Alam, S. K. et al. DARPP-32 promotes ERBB3-mediated resistance to molecular targeted therapy in EGFR-mutated lung adenocarcinoma. *Oncogene* **41**, 83–98 (2021).
35. Avanes, A., Lenz, G. & Momand, J. Darpp-32 and t-Darpp protein products of PPP1R1B: Old dogs with new tricks. *Biochem. Pharmacol.* **160**, 71–79 (2019).
36. Lenz, G. et al. t-Darpp activates IGF-1R signaling to regulate glucose metabolism in trastuzumab-resistant breast cancer cells. *Clin. Cancer Res.* **24**, 1216–1226 (2017).
37. Zhu, S., Belkhir, A. & El-Rifai, W. DARPP-32 increases interactions between epidermal growth factor receptor and ERBB3 to promote tumor resistance to gefitinib. *Gastroenterology* **141**, 1738–1748.e1731-1732 (2011).
38. Kwon, Y. G., Lee, S. Y., Choi, Y., Greengard, P. & Nairn, A. C. Cell cycle-dependent phosphorylation of mammalian protein phosphatase 1 by cdc2 kinase. *Proc. Natl Acad. Sci. USA* **94**, 2168–2173 (1997).
39. Hansen, C. et al. Wnt-5a-induced phosphorylation of DARPP-32 inhibits breast cancer cell migration in a CREB-dependent manner. *J. Biol. Chem.* **284**, 27533–27543 (2009).
40. Mitsuhashi, S. et al. Usage of tautomycin, a novel inhibitor of protein phosphatase 1 (PP1), reveals that PP1 is a positive regulator of Raf-1 in vivo. *J. Biol. Chem.* **278**, 82–88 (2003).
41. Akagi, T., Sasai, K. & Hanafusa, H. Refractory nature of normal human diploid fibroblasts with respect to oncogene-mediated transformation. *Proc. Natl Acad. Sci. USA* **100**, 13567–13572 (2003).
42. Schröfelbauer, B., Polley, S., Behar, M., Ghosh, G. & Hoffmann, A. NEMO ensures signaling specificity of the pleiotropic IKK β by directing its kinase activity toward I κ B α . *Mol. Cell* **47**, 111–121 (2012).
43. Hinz, M. & Scheidereit, C. The I κ B kinase complex in NF- κ B regulation and beyond. *EMBO Rep.* **15**, 46–61 (2014).
44. Hayden, M. S. & Ghosh, S. NF- κ B, the first quarter-century: remarkable progress and outstanding questions. *Genes Dev.* **26**, 203–234 (2012).
45. Chariot, A. The NF- κ B-independent functions of IKK subunits in immunity and cancer. *Trends Cell Biol.* **19**, 404–413 (2009).
46. Antonia, R. J., Hagan, R. S. & Baldwin, A. S. Expanding the view of IKK: new substrates and new biology. *Trends Cell Biol.* **31**, 166–178 (2021).
47. Cao, Y. et al. IKK α provides an essential link between RANK signaling and cyclin D1 expression during mammary gland development. *Cell* **107**, 763–775 (2001).
48. Bennett, L. et al. High IKK α expression is associated with reduced time to recurrence and cancer specific survival in oestrogen receptor (ER)-positive breast cancer. *Int. J. Cancer* **140**, 1633–1644 (2017).
49. Hao, L. et al. Notch-1 activates estrogen receptor- α -dependent transcription via IKK α in breast cancer cells. *Oncogene* **29**, 201–213 (2010).
50. Dan, H. C., Antonia, R. J. & Baldwin, A. S. PI3K/Akt promotes feedforward mTORC2 activation through IKK α . *Oncotarget* **7**, 21064–21075 (2016).
51. Girault, J. A. & Nairn, A. C. DARPP-32 40 years later. *Adv. Pharmacol.* **90**, 67–87 (2021).
52. Saidy, B. et al. PP1, PKA and DARPP-32 in breast cancer: a retrospective assessment of protein and mRNA expression. *J. Cell. Mol. Med.* **25**, 5015–5024 (2021).
53. Gu, L., Waliqany, S. & Kane, S. E. Darpp-32 and its truncated variant t-Darpp have antagonistic effects on breast cancer cell growth and herceptin resistance. *PLoS ONE* **4**, e6220 (2009).
54. Gu, L., Lau, S. K., Loera, S., Somlo, G. & Kane, S. E. Protein kinase A activation confers resistance to trastuzumab in human breast cancer cell lines. *Clin. Cancer Res.* **15**, 7196–7206 (2009).
55. Matos, B., Howl, J., Jerónimo, C. & Fardilha, M. Modulation of serine/threonine-protein phosphatase 1 (PP1) complexes: a promising approach in cancer treatment. *Drug Discov. Today* **26**, 2680–2698 (2021).
56. Felgueiras, J., Jerónimo, C. & Fardilha, M. Protein phosphatase 1 in tumorigenesis: is it worth a closer look? *Biochim. Biophys. Acta Rev. Cancer* **1874**, 188433 (2020).
57. Jones, G. G. et al. SHOC2 phosphatase-dependent RAF dimerization mediates resistance to MEK inhibition in RAS-mutant cancers. *Nat. Commun.* **10**, 2532 (2019).
58. Wang, Z. et al. Protein 4.1N acts as a potential tumor suppressor linking PP1 to JNK-c-Jun pathway regulation in NSCLC. *Oncotarget* **7**, 509–523 (2015).
59. Cirak, Y. et al. Zoledronic acid in combination with serine/threonine phosphatase inhibitors induces enhanced cytotoxicity and apoptosis in hormone-refractory prostate cancer cell lines by decreasing the activities of PP1 and PP2A. *BJU Int.* **110**, E1147–E1154 (2012).
60. Singal, G. et al. Association of patient characteristics and tumor genomics with clinical outcomes among patients with non-small cell lung cancer using a clinicogenomic database. *JAMA* **321**, 1391–1399 (2019).
61. Ramadass, V., Vaiyapuri, T. & Tergaonkar, V. Small molecule NF- κ B pathway inhibitors in clinic. *Int. J. Mol. Sci.* **21**, 5164 (2020).
62. Engelman, J. A. et al. MET amplification leads to gefitinib resistance in lung cancer by activating ERBB3 signaling. *Science* **316**, 1039–1043 (2007).
63. Hata, A. N. et al. Tumor cells can follow distinct evolutionary paths to become resistant to epidermal growth factor receptor inhibition. *Nat. Med.* **22**, 262–269 (2016).
64. Song, K. A. et al. Epithelial-to-mesenchymal transition antagonizes response to targeted therapies in lung cancer by suppressing BIM. *Clin. Cancer Res.* **24**, 197–208 (2018).
65. Chen, Z. et al. Gastric tumour-derived ANGPT2 regulation by DARPP-32 promotes angiogenesis. *Gut* **65**, 925–934 (2016).
66. Alam, S. K. et al. DNA damage-induced ephrin-B2 reverse signaling promotes chemoresistance and drives EMT in colorectal carcinoma harboring mutant p53. *Cell Death Differ* **23**, 707–722 (2016).
67. Reya, T. et al. A role for Wnt signalling in self-renewal of haematopoietic stem cells. *Nature* **423**, 409–414 (2003).
68. Stewart, S. A. et al. Lentivirus-delivered stable gene silencing by RNAi in primary cells. *RNA* **9**, 493–501 (2003).
69. Nakano, H. et al. Differential regulation of I κ B kinase α and β by two upstream kinases, NF- κ B-inducing kinase and mitogen-activated protein kinase/ERK kinase-1. *Proc. Natl Acad. Sci. USA* **95**, 3537–3542 (1998).
70. Martz, C. A. et al. Systematic identification of signaling pathways with potential to confer anticancer drug resistance. *Sci. Signal* **7**, ra121 (2014).
71. Wang, L. et al. Suppressing STAT3 activity protects the endothelial barrier from VEGF-mediated vascular permeability. *Dis. Model Mech.* **14**, dmm049029 (2021).

ACKNOWLEDGEMENTS

This work was supported by a Research Scholar Grant RSG-21-034-01-TBG from the American Cancer Society, a Windfeldt Cancer Research Award, the Elsa U. Pardee Foundation, and The Hormel Foundation (to L.H.H.) as well as the Fifth District Eagles Cancer Telethon Postdoctoral Fellowship Award (to S.K.A.). We thank Sam Hagan and Brianna Kriesel for providing assistance with culturing cells, immunoblotting studies, and plasmid preparations. We thank Naomi Ruff for suggesting helpful manuscript revisions. We are grateful to Wael El-Rifai for sharing DARPP-32 plasmids, Georgiy Aslanidi for sharing expression plasmids, and Pasi A. Jänne, Aaron N. Hata, and Anthony C. Faber for generously providing NSCLC cells. We thank The Hormel Institute and its staff for administrative, shared equipment, animal facility, and institutional support. We appreciate the data acquisition assistance provided by Todd Schuster and Tanner Conway.

AUTHOR CONTRIBUTIONS

S.K.A. conducted in vitro cell line-based experiments, including immunoprecipitation experiments, soft-agar colony formation assays, and in vitro kinase and phosphatase assays. S.K.A. and L.H.H. managed the immunocompromised SCID/NCr mouse colony and performed tumor studies in mice. S.K.A. and L.W. conducted murine in vivo bioluminescence imaging and necropsy. L.W. purified full-length and truncated DARPP-32 protein from mammalian cells. S.K.A. and Z.Z. performed western blotting experiments. Z.Z. assisted with imaging and analysis of soft-agar colony formation assays. S.K.A., L.W., and L.H.H. provided technical and scientific support. S.K.A. and L.H.H. performed experimental troubleshooting, reviewed relevant scientific literature, critically analyzed data, prepared figures, and wrote the manuscript. L.H.H. conceived the aims, led the project, and acquired funding to complete the reported research. All authors approved the final version of this manuscript.

COMPETING INTERESTS

The authors declare no competing interests.

ADDITIONAL INFORMATION

Supplementary information The online version contains supplementary material available at <https://doi.org/10.1038/s41698-023-00370-3>.

Correspondence and requests for materials should be addressed to Sk. Kayum Alam or Luke H. Hoepfner.

Reprints and permission information is available at <http://www.nature.com/reprints>

Publisher's note Springer Nature remains neutral with regard to jurisdictional claims in published maps and institutional affiliations.



Open Access This article is licensed under a Creative Commons Attribution 4.0 International License, which permits use, sharing, adaptation, distribution and reproduction in any medium or format, as long as you give appropriate credit to the original author(s) and the source, provide a link to the Creative Commons license, and indicate if changes were made. The images or other third party material in this article are included in the article's Creative Commons license, unless indicated otherwise in a credit line to the material. If material is not included in the article's Creative Commons license and your intended use is not permitted by statutory regulation or exceeds the permitted use, you will need to obtain permission directly from the copyright holder. To view a copy of this license, visit <http://creativecommons.org/licenses/by/4.0/>.

© The Author(s) 2023